TOWARDS MULTI-SCALE NONLINEAR (AND LINEAR) SYSTEM IDENTIFICATION IN STRUCTURAL DYNAMICS

Young-Sup Lee[3], Alexander F. Vakakis[1], Gaetan Kerschen[2], D. Michael McFarland[3], Lawrence A. Bergman[3]

[1]Faculty of Applied Mathematical and Physical Science
National Technical University of Athens
P.O.BOX 64042, GR-157 10 Zografos, Athens, Greece
vakakis@central.ntua.gr

[2]Aerospace and Mechanical Engineering Department (LTAS),
University of Liege, Belgium; g.kerschen@ulg.ac.be

[3]Department of Aerospace Engineering,
University of Illinois at Urbana – Champaign, USA;
yslee4@uiuc.edu, dmmcf@uiuc.edu, lbergman@uiuc.edu

Keywords: Multi-scale system identification, Hilbert – Huang Transform, Wavelet transform

Abstract. *The Hilbert-Huang transform (HHT) has been shown to be effective for characterizing a wide range of nonstationary signals in terms of elemental oscillatory components, termed the intrinsic mode functions (IMFs). In this presentation, we describe a combination of methods involving numerical integral transforms and theoretical analysis that cumulate to a new nonparametric method for nonlinear system identification based on multiple slow-fast partitions of the dynamics. This method can find wide applicability to linear and (weakly or strongly) nonlinear systems with various damping and/or stiffness nonlinearities. Moreover, through this method we can systematically examine transient resonance captures in the responses of dynamically interacting nonlinear structures, hence, decomposing and identifying the underlying multimodal nonlinear modal interactions that give rise to complex phenomena.*

1 INTRODUCTION

The idea of using slow-flow dynamics for nonlinear system identification dates back to Feldman [1,2] who exploited the Hilbert transform. The proposed procedure is one of the most successful approaches to tracking the varying nature of vibration of a large class of nonlinear systems thanks to the extraction of backbone curves from experimental data. Alternative approaches for slow flow-based identification were developed, in particular the Wigner-Ville approach [3] and the wavelet transform [4,5] Using the Gabor transform, Bellizzi et al.[6] related the slow-flow dynamics to the concept of coupled nonlinear modes. Because multicomponent signals do not admit a well-behaved Hilbert transform, the Hilbert-Huang transform (HHT) was introduced in [7]. It has been shown to be effective for characterizing a wide range of signals in terms of elemental components, termed intrinsic mode functions (IMFs), through what has been called the empirical mode decomposition (EMD). Several applications of this technique to structural dynamics recently appeared [8-10].

The strength of the HHT lies in its ability to deal with nonlinear and nonstationary data, despite the absence of a serious analytical foundation under those assumptions. In this paper, we attempt to provide a fundamental understanding of the HHT in nonlinear structural dynamics by linking its outcome to the slow-flow dynamics. The slow-flow model is established by performing a partition between slow and fast dynamics using the complexification-averaging technique, and a dynamical system described by slowly-varying amplitudes and phases is obtained. These variables can also be extracted directly from the experimental measurements using the Hilbert transform coupled with the EMD. The comparison between the experimental and analytical results forms the basis of a nonlinear system identification method, termed the *slow-flow model identification (SFMI) method*.

2 WAVELET / HILBERT-HUANG TRANSFORM (WT/HTT) MULTI-SCALE NONLINEAR SYSTEM IDENTIFICATION

We demonstrate the basic aspects of the techniques and algorithms comprising the proposed nonlinear system identification method by considering two examples. The first example concerns a linear elastic system with an essentially nonlinear boundary attachment. Specifically, we consider a linear elastic rod of mass distribution M and length L resting on an elastic foundation with distributed stiffness k and distributed viscous

damping δ, and coupled to an ungrounded, lightweight end attachment of mass m<<M by means of an essentially nonlinear cubic stiffness of constant C, in parallel to a viscous damper ελ (cf. Figure 1). Assuming that the left boundary of the rod is clamped, that a transient external force F(t) is applied at position $x = d$ of the rod (where x is measured from the left clamped end of the rod), and that the system is initially at rest, the governing equations of motion are given by:

$$EA\frac{\partial^2 u(x,t)}{\partial x^2} - k\,u(x,t) - \delta\frac{\partial u(x,t)}{\partial t} + F(t)\,\delta(x-d) - C\left[u(L,t)-v(t)\right]^3\,\delta(x-L)$$
$$-\varepsilon\lambda\left[\frac{\partial u(L,t)}{\partial t} - \dot{v}(t)\right]\delta(x-L) = M\frac{\partial^2 u(x,t)}{\partial t^2}, \quad 0 \le x \le L, \qquad u(0,t) = 0$$
$$C\left[u(L,t)-v(t)\right]^3 + \varepsilon\lambda\left[\frac{\partial u(L,t)}{\partial t} - \dot{v}(t)\right] = m\ddot{v}(t)\ , \ u(x,0) = 0, \ \frac{\partial u(x,0)}{\partial t} = 0, \ v(0) = 0, \ \dot{v}(0) = 0 \qquad (1)$$

The equations of motions were numerically solved with Matlab by employing a finite element (FE) formulation and an implicit time integration scheme based on an adapted Newmark algorithm. To ensure proper spatial discretization, a total of 501 FE was used; moreover, the sampling frequency was selected to account for 122 modes of the rod oscillation. At each time step of the numerical integration the total energy balance was computed in order to ensure that, (a) the relative energy error between subsequent steps of the computation was less than 0.001%, and (b) that the error on the conservation of the total energy was less than 1%. The parameters were assigned the values, $L = 1$, $EA = 1.0$, $M = 1.0$, $\delta = 0.05$, $m = 0.1$, $\varepsilon = 0.1$, $\lambda = 0.5$, and the transient (shock) excitation was chosen to be a half sine pulse of amplitude F and duration $0.1T_1$, where T_1 is the period of the first mode of the linear rod; the shock is applied at position $d = 0.3$ on the rod.

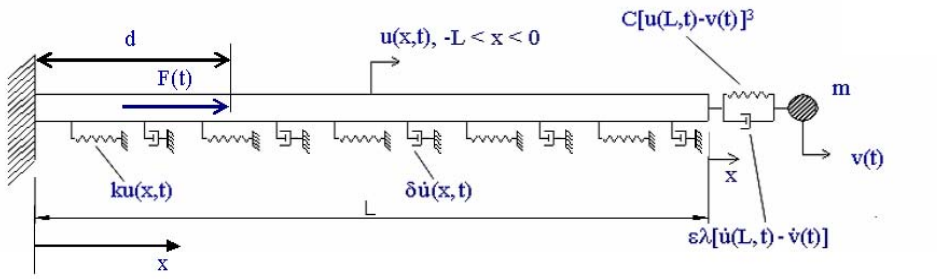

Figure 1. Linear rod with essentially nonlinear boundary attachment.

Post processing of the numerically computed time series of the rod and the NES was performed by two different techniques. First, the transient data was analyzed by *Wavelet Transforms (WT)* employing a Matlab-based algorithm developed at Université de Liège by Dr.V.Lenaerts in collaboration with Dr.P.Argoul from the 'Ecole Nationale des Ponts et Chaussees' [5]. Although the algorithm provides the opportunity to use two kinds of mother wavelets, namely Morlet and Cauchy, in the applications presented herein only the Morlet mother wavelet has been used; this is a Gaussian-windowed complex sinusoid of frequency ω_0 (in rad/sec), $\psi_M(t) = e^{-t^2/2}\,e^{j\omega_0 t}$. The frequency ω_0 is the user parameter which enables one to tune the frequency and time resolution of the results. Occasionally the signals were divided in two phases (early- and late-phase) for the application of the WT, since as the amplitudes get smaller with respect to their initial values the corresponding wavelet traces are too light to be visible. The WT contour plots (WT spectra) depict the amplitude of the WT of the signal as function of frequency (vertical axis) and time (horizontal axis). Heavy shaded areas correspond to regions where the amplitude of the WT is high, whereas lightly shaded ones correspond to low amplitudes of the WT. Such plots enable one to deduce the temporal evolutions of the dominant frequency components of the signals analyzed, as well as, transitions between different modes that participate in the transient nonlinear responses.

Further analysis of the numerical time series was performed using a combination of *Empirical Mode Decomposition (EMD)* and *Hilbert Transform* (the so called *Hilbert-Huang Transform - HTT*). HHT is a method to decompose a signal (time series) in terms components called *Intrinsic Mode Functions (IMFs)* [7]. The IMFs satisfy the following three main conditions:

- For the duration of the entire time series, the number of extrema and of zero crossings of each IMF should either be equal or differ at most by one

- At any given time instant, the mean value (moving average) of the local envelopes of the IMFs defined by their local maxima and minima should be zero
- The superposition of all IMFs should reconstructs the time series

Hence, EMD analysis extracts oscillating modulations or modes imbedded in the data. It follows that *the essence of the EMD method is to empirically identify the intrinsic oscillatory modes in the data (time series), and to categorize them in terms of their characteristic time scales, by considering the successive extreme values of the signal.* The IMFs have usually a physical interpretation as far as their characteristic scales are concerned (indeed, as shown below, certain IMFs possess instantaneous frequencies that are nearly identical to resonance frequencies of the rod or the NES); but this need not always be the case. This implies that certain IMFs may represent artificial (non-physical) oscillating modes of the data. Moreover, by Hilbert – transforming the IMFs one computes temporal evolutions of their instantaneous amplitudes and frequencies, which, in turn, can be used for the construction of the Hilbert spectrum of the signal [7]. Nevertheless there are cases where at a certain time scale a transient phenomenon is intermittent – for example, turbulence in fluid motion, and in these cases the decomposed components could contain two scales embedded in a single IMF component, and an intermittency criterion should be adopted during the decomposition of the signal.

Two simulations are studied in detail: Application 1 corresponds to $C = 0.8,\ F = 10.0$, whereas Application 2 corresponds to $C = 5.0,\ F = 100.0$. What distinguishes the two applications is the amount of *targeted energy transfer (TET)* from the directly forced rod to the nonlinear attachment. This energy transfer is quantified by computing the energy measure η, defined as,

$$\eta \equiv \lim_{t>>1} \frac{\int_0^t \varepsilon\lambda\left[\dot{v}(\tau) - \frac{\partial u(L,\tau)}{\partial \tau}\right]^2 d\tau}{\int_0^T F(\tau)\frac{\partial u(d,\tau)}{\partial \tau}\, d\tau} \tag{2}$$

This measure represents the portion of input energy to the rod transferred and passively dissipated by the viscous damper of the nonlinear attachment. For Application 1 there is strong TET as $\eta = 0.71$ (the closer η is to unity, the stronger is the TET from the rod to the attachment), and the nonlinear attachment acts, in essence as *nonlinear energy sink (NES).* For Application 2 there is weak TET since $\eta = 0.51$. We will show that by employing the previous post processing techniques it is possible to perform multi-scale identification of the nonlinear modal interactions that govern the strength of TET in this system.

In Figure 2a we present IMF – based reconstructions of the transient responses of the edge of the rod and the nonlinear attachment for Application 1; complete agreement between numerical simulation and IMF – based reconstruction is observed, proving the capacity of the HHT analysis to decompose the transient nonlinear responses through IMFs. Representative IMFs are depicted in Figure 2b. Next, decompositions of the IMFs in terms of their instantaneous amplitudes and phases were performed in order to examine their individual frequency contents. This information should be analyzed together with the corresponding WT spectrum of the relative transient response between the edge of the rod and the NES which appears in Figure 2c. From the wavelet plot it is clearly observed that strong TET in this Application is associated with a low frequency 'locking' of the dynamics to a nonlinear mode below the first eigenfrequency of the rod (0.29 Hz). In Figure 2d we depict the instantaneous frequencies of the dominant 2^{nd} IMF of the attachment response, and the dominant 9^{th} IMF of the rod end response, superimposed to the wavelet spectra of the respective numerical time series. Several conclusions can be drawn from these results:

(i) It is clear that the 2^{nd} IMF of the attachment and the 9^{th} IMF of the rod possess nearly constant instantaneous frequencies precisely at the low frequency range of the nonlinear mode of the WT spectrum of Figure 2c; hence, these IMFs engage in 1:1 resonance capture in the initial (high energy) stage of the transient dynamics. It is precisely such resonance captures that lead to passive targeted energy pumping from the rod to the NES, as quantified by the energy dissipation measure η. Moreover, *the fact that the described 1:1 resonance capture takes place in the early stage of the dynamics where the energy of the system is high, explains the strong TET observed in this Application.*

(iii) In the mentioned resonance capture regime, the 2^{nd} (dominant) IMF of the rod coincides in frequency with the dominant harmonic component of the transient response of the NES, whereas the 9^{th} IMF of the rod coincides with the lowest of the dominant harmonic components of the transient response of the edge of the rod.

These results (together with the ones presented below) demonstrate the capacity of the WT/HTT analysis to accurately detect the oscillatory components of the rod and NES time series that engage in resonance capture, and, are responsible for the passive energy pumping phenomena from the rod to the NES.

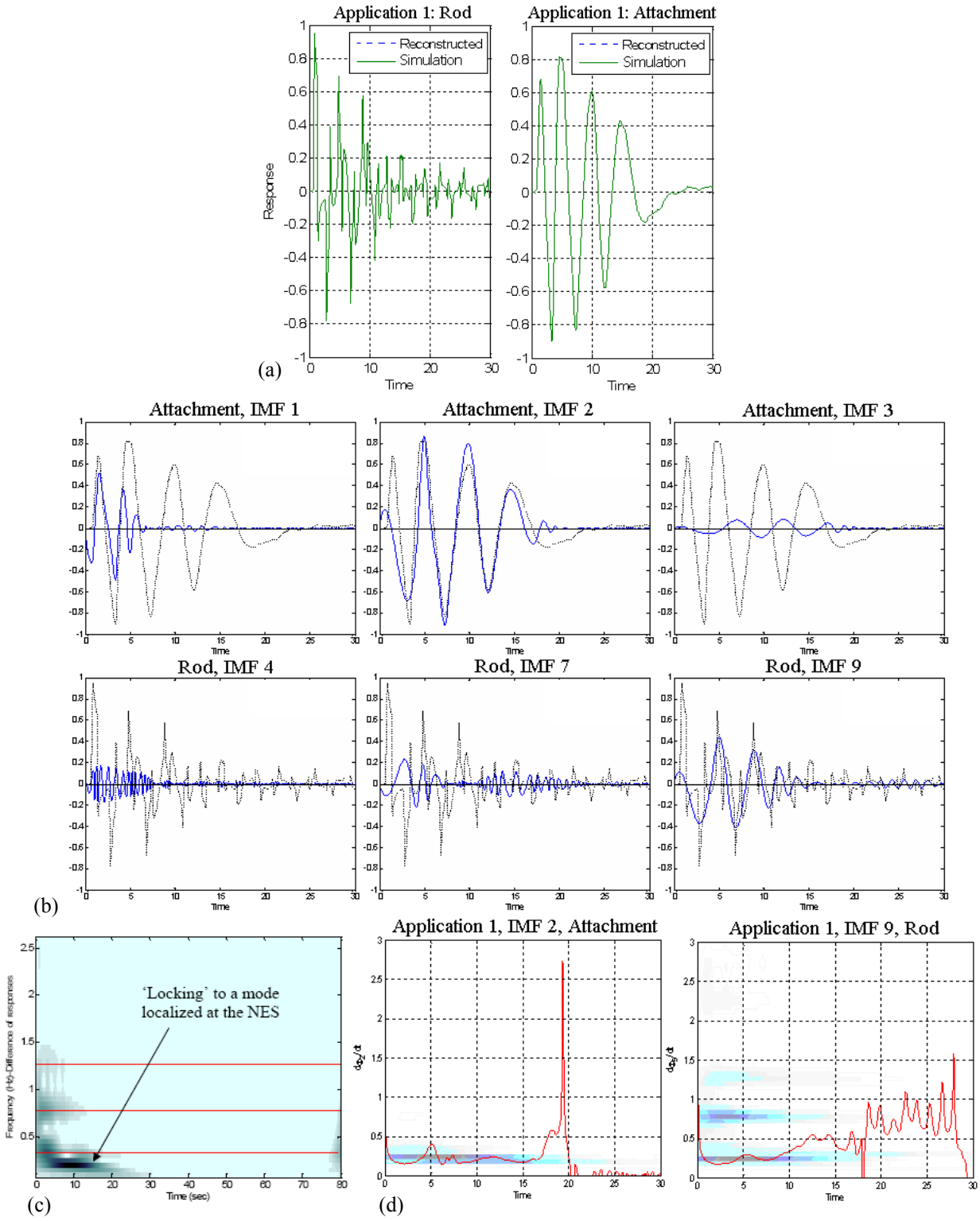

Figure 2. Application 1, strong TET: (a) Time series, (b) dominant IMFs of the rod and attachment responses, (c) wavelet spectrum of the relative response between attachment and rod, (d) IMF frequencies.

In Figure 3a we depict the simulated and IMF – based reconstructed responses for Application 2 – weaker

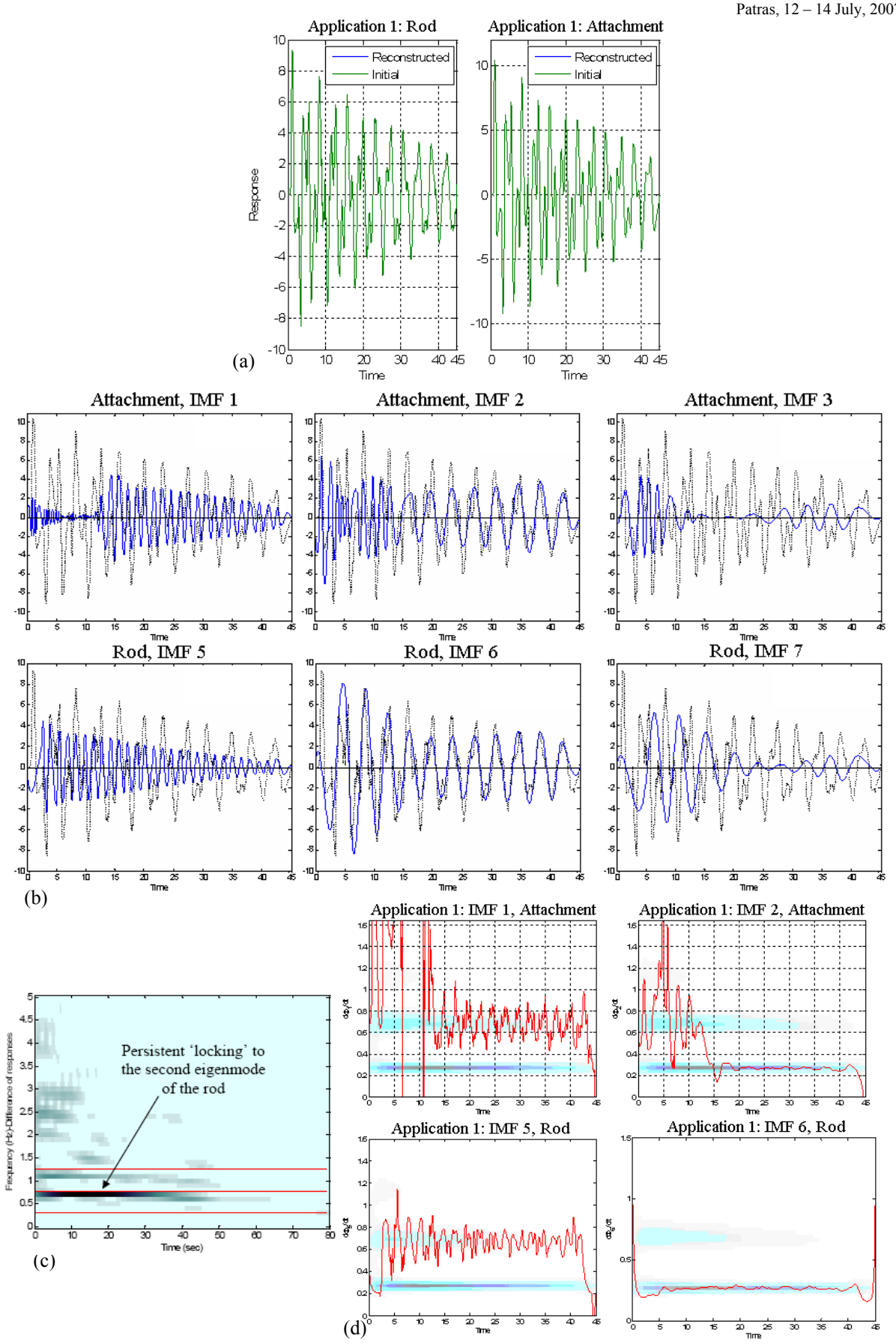

Figure 3. Application 2, weak TET: (a) Time series, (b) dominant IMFs of the rod and attachment responses, (c) wavelet spectrum of the relative response between attachment and rod, (d) IMF frequencies.

targeted energy pumping, from which again complete agreement between simulations and IMF – reconstructions is observed. Representative IMFs of the early (high energy) responses of the edge of the rod and the attachment are depicted in Figure 3b. Consideration of the resonance interactions between the IMFs of the rod and the attachment reveals the reason behind the weak targeted energy pumping in this Application. Referring to the WT spectrum of the relative response between the edge of the rod and the NES for this Application (cf. Figure 3c), we clearly note the 'locking' of the dynamics in the vicinity of the second linearized eigenfrequency of the rod (close to 0.77 Hz). Examining the temporal evolutions of the instantaneous frequencies of the IMFs of the early transient responses of the edge of the rod and the NES in Figure 3d, we note that the 1st IMF of the attachment and the 5th IMF of the rod develop delayed frequency 'plateaus' close to 0.77 Hz for $t > 12$; this indicates a clear 1:1 resonance capture between these two IMFs. However, since this resonance capture occurs at a *later stage of the response* (e.g., at a stage where a significant portion of the initial energy of the system has already been dissipated due to damping), the resulting targeted energy pumping from the rod to the NES is not as strong as in the previously discussed Application 1, where the corresponding resonance capture takes place at the critical early stage of the motion where the energy of the system is at its highest level. In Figure 3 we also show that in Application 2 there occurs an additional 'delayed' 1:1 resonance capture between the 2nd IMF of the attachment and the 6th IMF of the edge of the rod at a frequency near the first eigenfrequency of the rod (0.29 Hz), which, however, does not lead to significant energy transfer from the rod to the NES. Finally, from Figure 3d we note that, by superimposing the instantaneous IMF frequencies to the WT spectra of the respective numerical time series, we infer that the 1st and 2nd IMFs of the nonlinear attachment coincide with the higher and lower dominant harmonics, respectively, of the time series of the nonlinear attachment, but only during the later stage of the motion. Similar conclusions can be drawn with regard to the 5th and 6th IMF of the rod.

The previous results demonstrate the capacity of the combined WT/HHT technique to identify the dominant oscillatory components governing strongly nonlinear modal interactions, as well as the time scales at

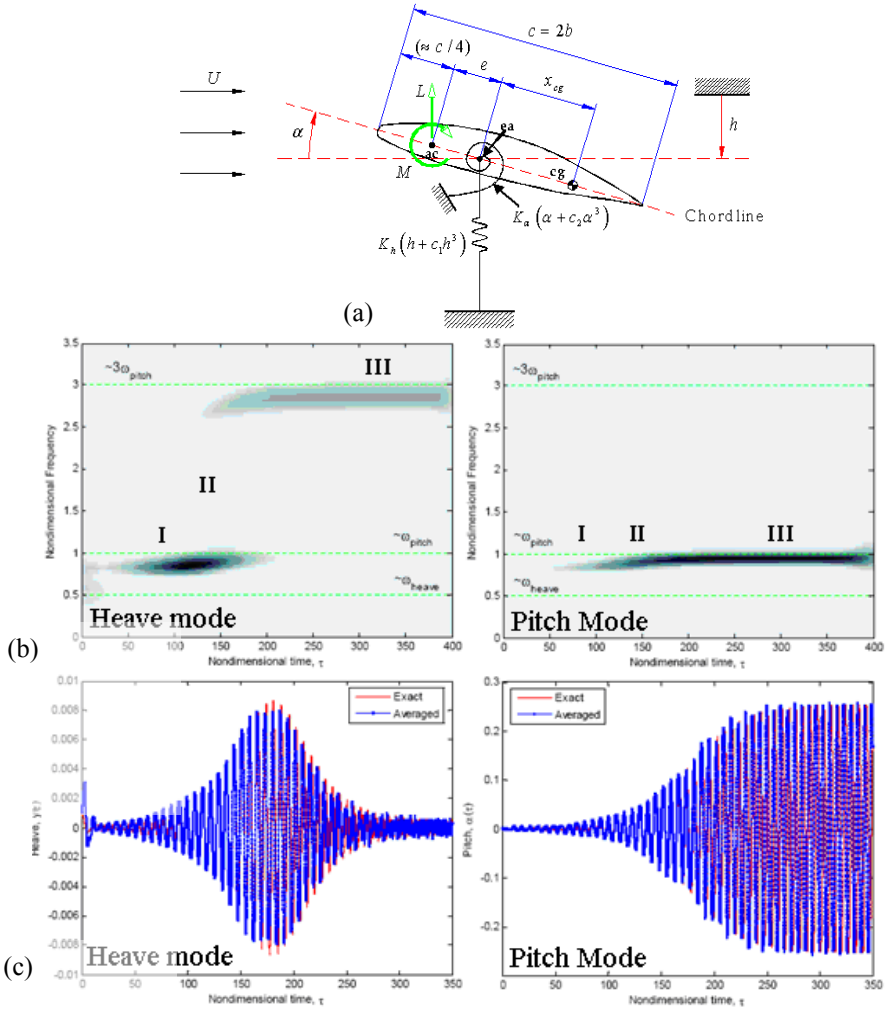

Figure 4. LCO in an in-flow rigid wing: (a) configuration, (b) wavelet spectra of the pitch and heave responses, (c) comparisons between direct numerical simulations and reduced order dynamics [11].

which these modal interactions occur. We further demonstrate the method, by identifying the nonlinear modal interactions that lead to aeroelastic instabilities (limit cycle oscillations – LCOs) an in-flow rigid wing. We

consider two degrees-of-freedom for the wing, namely, heave and pitch (Figure 4a), and assume cubic structural nonlinearities in both DOFs and quasi-steady aerodynamics. In Figure 4b we depict the responses of the heave and pitch modes when LCO develops at supercritical speed, together with their Morlet wavelet transforms (WT), which provide information on the temporal evolution of the dominant harmonic components of the transient responses of the modes of the wing. This enables us to clearly identify and study the resonant modal interactions and transitions that occur at different stages of LCO formation. In Figure 4c we depict the transient responses of the reduced order model resulting from the system identification of the nonlinear modal interactions between flow, pitch and heave, from which an accurate prediction of the dynamics is inferred.

The WT of the transient dynamics reveal the following three stages of LCO formation:

Stage I: Energy increases in both pitch and heave modes of the wing as energy is fed from the flow to the heave and pitch modes through 1:1 transient resonance capture (RC) (e.g., the instantaneous frequencies of heave and pitch modes are nearly equal); in this case the heave mode behaves as a 'nonlinear energy source' driving the pitch mode.

Stage II: Once the heave mode reaches its maximum amplitude, escape from 1:1 RC occurs, and the energy of the heave mode is almost entirely transferred to the pitch mode.

Stage III: The LCO is fully developed as a steady state motion is reached, and a 3:1 permanent resonance capture occurs.

These stages constitute the LCO triggering mechanism for the rigid wing, composed of an initial 1:1 transient resonance capture between heave and pitch, followed by escape from capture, and then 3:1 permanent resonance capture. This analysis reveals the existence of three basic frequencies (or equivalently, time scales) in the dynamics: the linearized frequencies of the heave and pitch modes, ω_{heave}, ω_{pitch}, respectively, and a frequency three times the linearized pitch frequency, $3\omega_{pitch}$. Hence, the dominant time scales of the dynamics that govern LCO development are identified in this example as well.

3 REDUCED ORDER MODELING BASED ON SLOW-FAST PARTITIONS OF THE DYNAMICS

Based on the previous decompositions, we proceed to construct a reduced order model of the nonlinear transient dynamics governing LCO formation in the in-flow wing by expressing the heave and pitch transient responses as summations of slow modulations of fast-varying oscillations possessing the three dominant time scales. We will refer to this approach as *Complexification and Averaging (CxA)* technique. To this end, the heave and pitch responses, $y(t)$ and $\alpha(t)$, respectively, are decomposed into the form,

$$y(t) = y_1(t) + y_2(t) + y_3(t), \quad \alpha(t) = \alpha_1(t) + \alpha_2(t) + \alpha_3(t) \tag{3}$$

where each term is represented as a 'slowly varying' modulation of a 'fast' oscillation with frequency equal to one of the aforementioned dominant harmonics. Hence, we introduce a simultaneous slow/fast partition of the dynamics at the dominant (three) time scales of the problem. Mathematically, we introduce the new complex variables,

$$\begin{array}{lll} \psi_1 = \dot{y}_1 + j\omega_{heave} y_1, & \psi_3 = \dot{y}_2 + j\omega_{pitch} y_2, & \psi_5 = \dot{y}_3 + 3j\omega_{pitch} y_3, \\ \psi_2 = \dot{\alpha}_1 + j\omega_{heave} \alpha_1, & \psi_4 = \dot{\alpha}_2 + j\omega_{pitch} \alpha_2, & \psi_6 = \dot{\alpha}_3 + 3j\omega_{pitch} \alpha_3 \end{array} \tag{4}$$

where $j = (-1)^{1/2}$. Expressing the original real variables of the problem and their derivatives in terms of ψ_p (e.g., $y = (1/2j\omega_{heave})(\psi_1 - \overline{\psi}_1) + (1/2j\omega_{pitch})(\psi_3 - \overline{\psi}_3) + (1/6j\omega_{pitch})(\psi_5 - \overline{\psi}_5)$, and so on), and substituting into the equations of motion, we obtain a set of complex equations. We now introduce the slow/fast partition,

$$\begin{array}{lll} \psi_1 = \phi_1(t) e^{j\omega_{heave} t}, & \psi_3 = \phi_3(t) e^{j\omega_{pitch} t}, & \psi_5 = \phi_5(t) e^{3j\omega_{pitch} t} \\ \psi_2 = \phi_2(t) e^{j\omega_{heave} t}, & \psi_4 = \phi_4(t) e^{j\omega_{pitch} t}, & \psi_6 = \phi_6(t) e^{3j\omega_{pitch} t} \end{array} \tag{5}$$

where the complex functions $\phi_p(t)$ are 'slow' modulations multiplying 'fast' oscillations (represented by the complex exponentials) at the different time scales of the problem. The 'slow' modulations $\phi_p(t)$ govern the essential dynamics through a set of slow-flow equations which are derived by applying multiphase averaging over the 'fast' frequency components $e^{j\omega_{heave} t}$, $e^{j\omega_{pitch} t}$ and $e^{3j\omega_{pitch} t}$, respectively. This set has the form,

$$\underline{\dot{\phi}} + \underline{F}(\underline{\phi}; \underline{\mu}) = \underline{0}, \quad (\underline{\phi}, \underline{\mu}) \in R^6 \times R^M \tag{6}$$

and represents the essential (important) dynamics of the system after the (trivial) fast oscillatory components at different time scales are averaged out (the M-vector $\underline{\mu}$ represents the parameters of the problem). The slow-flow reduction (6) accurately regenerates the transient measurements (see Figure 4c), and in addition it explicitly captures the qualitative and quantitative dynamics of the system (e.g., bifurcations) [11,12].

Furthermore, as discussed in [13], the slow-flow CxA reduction provides a rigorous theoretical background for interpreting the results of the WT/HHT technique, and can form the basis of a nonparametric system

identification technique. Both the WT/HHT and CxA approaches share a common basis by expanding a multi-frequency signal in a series of simple, monocomponent oscillatory modes, which are related to the dominant frequency components of the signal: (i) The CxA method transforms the equations of motion of a nonlinear system into a set of approximate equations that govern the slow flow; there is no *a priori* restriction on the number of frequency components that can be taken into account in this formulation; (ii) The WT/HHT characterizes a signal through the envelope and phase of the elemental oscillatory components, the IMFs. Hence, the link between the methods is clear: The equations derived using the CxA method are identical to the equations governing the amplitude and phase of the modeled IMFs; the CxA method therefore provides a rigorous analytical framework for the WT/HHT.

5 CONCLUSIONS

We discussed the two ingredients of a new nonlinear system identification method, namely the WT/HHT technique coupled to CxA methodology. The method is based on multiple slow-fast partitions of the time series, and its basic advantage is that being based on the direct analysis of time-series it can be applied to general classes of nonlinear systems. Moreover, the method can be regarded as physics-based, as it has the capacity to decompose complex nonlinear modal interactions in terms of their dominant oscillatory processes, and to identify the specific time scales where the most essential nonlinear dynamics take place. As such, the propose dmethod holds promise to a nonparametric nonlinear system identification method of wide applicability.

REFERENCES

[1] Feldman, M. (1994), "Nonlinear system vibration analysis using the Hilbert transform - I. Free vibration analysis method FREEVIB", Mechanical Systems and Signal Processing, 8, pp. 119-127.

[2] Feldman, M. (1997), "Non-linear free vibration identification via the Hilbert transform", Journal of Sound and Vibration, 208, pp. 475-489.

[3] Feldman, M., Braun, S. (1995), "Identification of non-linear system parameters via the instantaneous frequency: application of the Hilbert transform and Wigner-Ville technique," *Proceedings of the 13th International Modal Analysis Conference (IMAC)*, Nashville, pp. 637-642.

[4] Staszewski, W.J. (1998), "Identification of non-linear systems using multi-scale ridges and skeletons of the wavelet transform," Journal of Sound and Vibration, 214, pp. 639-658.

[5] Argoul, P. and Le, T.P. (2003), "Instantaneous indicators of structural behaviour based on the continuous Cauchy wavelet analysis," Mechanical Systems and Signal Processing, 17, pp. 243-250.

[6] Bellizzi, S., Gullemain, P. and Kronland-Martinet, R. (2001), "Identification of coupled non-linear modes from free vibration using time-frequency representation," Journal of Sound and Vibration, 243, pp. 191-213.

[7] Huang, N.E., Shen, Z., Long, S.R., Wu, M.C., Shih, H.H., Zheng, Q., Yen, N.C., Tung, C.C. and Liu, H.H. (1998), "The empirical mode decomposition and the Hilbert spectrum for nonlinear and non-stationary time series analysis," *Proceedings of the Royal Society of London, Series A — Mathematical, Physical and Engineering Sciences*, Vol. 454, pp. 903-995.

[8] Yang, J.N., Lei, Y., Pan, S.W. and Huang, N. (2003), "System identification of linear structures based on Hilbert-Huang spectral analysis; Part 1: Normal modes," Earthquake Engineering and Structural Dynamics, 32, pp. 1443-1467.

[9] F. Georgiades (2006), *Nonlinear Localization and Targeted Energy Transfer Phenomena in Vibrating Systems with Smooth and Non-smooth Stiffness Nonlinearities,* PhD Thesis, School of Applied Mathematical and Physical Sciences, National Technical University of Athens.

[10] S. Tsakirtzis (2006), *Passive Targeted Energy Transfers from Elastic Continua to Essentially Nonlinear Attachments for Suppressing Dynamical Disturbances,* PhD Thesis, School of Applied Mathematical and Physical Sciences, National Technical University of Athens.

[11] Lee Y.S., A.F. Vakakis, L.A. Bergman, D.M. McFarland, and G. Kerschen (2005), "Triggering mechanisms of limit cycle oscillations due to aeroelastic instability," Journal of Fluids and Structures 21, pp. 485-529.

[12] Lee Y.S., A.F. Vakakis, L.A. Bergman, D.M. McFarland, G. Kerschen (2007), "Suppression of Aeroelastic Instability by Means of Broadband Passive Targeted Energy Transfers, Part I: Theory," AIAA Journal (in press).